Cancer Science
Japanese Cancer Association JCA
Open Access

Potential roles of microRNA-29a in the molecular pathophysiology of T-cell acute lymphoblastic leukemia

Lucila H. Oliveira,[1,3,6] Josiane L. Schiavinato,[2,3,6] Mariane S. Fráguas,[1,3,6] Antonio R. Lucena-Araujo,[4] Rodrigo Haddad,[5] Amélia G. Araújo,[1,3] Leandro F. Dalmazzo,[1] Eduardo M. Rego,[1,3] Dimas T. Covas,[1,3] Marco A. Zago[1,3] and Rodrigo A. Panepucci[1,2,3]

[1]Department of Internal Medicine, Medical School of Ribeirão Preto, University of São Paulo, São Paulo; [2]Department of Genetics, Medical School of Ribeirão Preto, University of São Paulo, São Paulo; [3]Center for Cell Based Therapy, Regional Blood Center, Ribeirão Preto; [4]Department of Genetics, Federal University of Pernambuco, Recife; [5]School of Ceilandia, University of Brasilia, Brasilia, Brazil

Key words

DNMT, epigenetic regulation, miR-29a, T-cell acute lymphoblastic leukemia, TET

Correspondence

Rodrigo Alexandre Panepucci, Fundação Hemocentro de Ribeirão Preto, Rua: Tenente Catão Roxo, 2501, CEP: 14051-140, Ribeirão Preto, São Paulo, Brazil.
Tel.: +55-16-3602-2223; Fax: +55-16-2101-9309;
E-mail: rapane@gmail.com

Funding Information

São Paulo Research Foundation (FAPESP); National Council for Scientific and Technological Development (CNPq); Funding Authority for Studies and Projects (FINEP), Brazil.

[6]These authors contributed equally to this work.

Received March 11, 2015; Revised July 8, 2015; Accepted August 3, 2015

Cancer Sci **106** (2015) 1264–1277

doi: 10.1111/cas.12766

Recent evidence has shown that deregulated expression of members of the microRNA-29 (miR-29) family may play a critical role in human cancer, including hematological malignancies. However, the roles of miR-29 in the molecular pathophysiology of T-cell acute lymphoblastic leukemia (T-ALL) has not been investigated. Here, we show that lower levels of miR-29a were significantly associated with higher blast counts in the bone marrow and with increased disease-free survival in T-ALL patients. Furthermore, miR-29a levels are extremely reduced in T-ALL cells compared to normal T cells. Microarray analysis following introduction of synthetic miR-29a mimics into Jurkat cells revealed the downregulation of several predicted targets (CDK6, PXDN, MCL1, PIK3R1, and CXXC6), including targets with roles in active and passive DNA demethylation (such as DNMT3a, DNMT3b, and members of the TET family and TDG). Restoring miR-29a levels in Jurkat and Molt-4 T-ALL cells led to the demethylation of many genes commonly methylated in T-ALL. Overall, our results suggest that reduced miR-29a levels may contribute to the altered epigenetic status of T-ALL, highlighting its relevance in the physiopathology of this disease.

MicroRNAs (miRNAs or miRs) are a class of small non-coding RNAs that exert pleiotropic effects by post-transcriptionally regulating multiple transcript targets involved in distinct cellular processes in both normal and pathological conditions.[1–4] Among the miRNAs described, contrasting findings reported altered levels of miR-29 family members (miR-29a, miR-29b, and miR-29c) in several types of human cancer.[5–9] Lower levels of the miR-29 family members were described in the more aggressive subtype of B-cell chronic lymphocytic leukemia (B-CLL) compared with the indolent subtype of B-CLL.[10,11] Furthermore, reduced expression levels of the miR-29 family members were also described in mantle cell lymphoma (MCL) and associated with a significantly short survival.[12] In contrast, miR-29a was found to be one of the most expressed miRNAs in CLL[13] and its forced expression in B-cells from mouse resulted in the development of leukemia with B-CLL characteristics. Additionally, ectopic expression of miR-29a in mouse hematopoietic stem cells (HSC) promoted self-renewal of myeloid progenitors, leading to a myeloproliferative disorder and, ultimately, to acute myeloid leukemia (AML).[14] Despite several reports describing the role of miR-29 family members in hematological malignancies, their potential involvement in T-cell acute lymphocytic leukemia (T-ALL) is still elusive.

We explored the potential roles of miR-29a in T-ALL, through the introduction of synthetic miR-29a mimics into Jurkat cells followed by whole transcriptome analysis. Our strategy allowed the identification of previously described miR-29 targets, including central components of DNA methylation (DNA methyltransferase 3a [DNMT3a] and DNMT3b). Evaluation of the epigenetic effects in transfected Jurkat and Molt-4 T-ALL cell lines revealed that miR-29a promotes the demethylation of many genes commonly methylated in T-ALL, functionally linking miR-29a to the altered epigenetic status of T-ALL. Finally, we identified a significant association of miR-29a levels with blast counts and with disease-free survival in T-ALL patients, highlighting the relevance of miR-29 in the physiopathology of T-ALL.

Material and Methods

Evaluation of miR-29a expression in microRNA.org database. In order to evaluate how miR-29a levels in T-ALL cells compare to those of normal cells, we used miRNA expression data

downloaded from microRNA.org. The libraries derived from a $CD34^+$ HSC sample, a Jurkat leukemic T-cell line, and all libraries generated from normal T-cells or T-ALL samples were selected for the comparison. The values were presented in decreasing order of expression.

Cell culture and transfection with synthetic miRNAs. The human Jurkat T, Molt-4, and CCRF-Cem cell lines were grown in RPMI-1640 (Gibco, Invitrogen, Merelbeke, Belgium) supplemented with 20% FCS (HyClone, Perbio, Belgium), 50 U/mL penicillin and 50 μg/mL streptomycin at 37°C and 5% CO_2. Cells were transfected with synthetic RNA molecules corresponding to miR-29a mimics (pre-miR-29a) or control miR (pre-miR-ctrl) (Ambion, Austin, TX, USA).

For microarray and methylation-specific PCR (MS-PCR), 1×10^6 cells were electroporated at a final concentration of 100 nM, using the Neon transfection system (Invitrogen, Carlsbad, CA, USA), according to the manufacturer's instructions. Briefly, the Jurkat cells were pulsed three times (1400 V, 10 ms), resulting in an efficiency and viability of 80%. Cells were maintained in RPMI medium + 10% FCS without antibiotics and harvested 48 h post-transfection for DNA and RNA extraction.

All the remaining experiments were carried using the DMRIE-C Transfection Reagent (Invitrogen), according to the manufacturer's instructions. Briefly, 1.5×10^5 cells were plated in 24-wells plates in 300 μL RPMI medium + 10% FCS without antibiotics. DMRIE-C reagent (0.5 μL/well) was mixed with Opti-MEM I Reduced Serum Medium (Invitrogen) by vortexing, and incubated at room temperature for 10 min. Next, control or miR-29a mimics were added (50 nM final concentration) and the vortexed mixture (100 μL) was further incubated for 15 min at room temperature, before being added to the cells. After 4 h, 600 μL RPMI medium + 10% FCS with antibiotics was added per well. For XTT and quantitative immunofluorescence microscopy experiments, 1.0×10^4 cells were transfected in 96-well plates in a final volume of 100 μL using 0.25 μL/well DMRIE-C. After 4 h, 100 μL RPMI medium + 10% FCS with antibiotics was added per well. Cells were assayed at different times following transfection (as further detailed elsewhere).

DNA and RNA isolation. Total RNA was extracted using the TRIzol LS reagent, according to the manufacturer's instructions (Invitrogen). RNA samples used for the microarrays experiments were purified with the RNeasy Kit (Qiagen, Valencia, CA, USA) and RNA quality was assessed by agarose gel electrophoresis trough 28S and 18S ribosomal RNA visualization. Genomic DNA was extracted using the Flexigene DNA kit, according to the manufacturer's instructions (Cat. 51206; Qiagen). Quantification was carried by spectrophotometry at 260 nM and the ratio of the absorbance at 260 and 280 nm (A260/280) was used to assess the purity of nucleic acids.

Oligonucleotide microarrays. Gene expression profiles were obtained using the commercially available Human Whole Genome Oligo Microarray Kit (Agilent Technologies, Palo Alto, CA, USA), according to the manufacturer's protocol and as previously described.[15] Microarray slides were scanned at 535 nm with 5 μm/pixel resolution using a DNA microarray scanner with SureScan high-resolution technology (Agilent Technologies) and the fluorescent intensities were determined by Feature Extraction software version 11.5 (Agilent Technologies). Expression values were normalized by the 75th percentile and used for further analysis. The data discussed in this publication have been deposited in NCBI's Gene Expression Omnibus[16,17] and are accessible through GEO Series accession number GSE48063 (http://www.ncbi.nlm.nih.gov/geo/query/acc.cgi?acc=GSE48063).

Bioinformatics analysis. Transcripts showing a downregulation of at least 10% in the Jurkat cell line transfected with pre-miR-29a (compared to pre-miR-ctrl) were selected and compared to the set of TargetScan predicted targets (release 6.2; www.targetscan.org).[18] Next, we used the DAVID Functional Annotation Tool (http://david.abcc.ncifcrf.gov/home.jsp) to identify pathways and biological processes statistically enriched for miR-29a targets and, thus, potentially modulated by this miR.[19,20]

Real-time quantitative PCR for gene expression analysis. Total RNA was reverse transcribed using the High Capacity cDNA Reverse Transcription Kit (Applied Biosystems, Foster City, CA, USA), according to the manufacturer's instructions. Gene expression quantitative PCR (qPCR) reactions were carried out in duplicate. Evaluations were carried out in an ABI Prism 7300 Sequence Detection System (Applied Biosystems) or a CFX96 Real-Time PCR (Bio-Rad, Hercules, CA, USA) and the Power SYBR Green Master Mix (Applied Biosystems). Real-time qPCR primers for ten-eleven-translocation (TET)1, TET2, TET3, DNMT1, DNMT3a, DNMT3b, ADCY5, LXH4, GFPT2, GIPC2, and AHR were designed using the RealTime qPCR online tool from IDT (Integrated DNA Technologies, Skokie, IL, USA). Primer sequences and cycling details for gene expression qPCR analysis can be found in Table S1. Patient samples were normalized using ACTB as the housekeeping gene. All remaining evaluations were normalized using GAPDH. The comparative Ct method[21] was used to calculate relative expression. For transfection experiments, the mean ΔCT value of control samples was used as a reference value. Expression values in T-ALL samples were obtained by using Jurkat cells as a reference sample.

Real-time qPCR for miRNA expression analysis. TaqMan assays were used for the quantitative expression analysis of the mature miRNA hsa-miR-29a (assay ID 002112) as well as the endogenous controls (RNU24 [assay ID 001001] and RNU48 [assay ID 001006]). Reverse transcription was carried out using a High Capacity cDNA Reverse Transcription Kit using 5 ng total RNA and specific stem–loop primers for each miRNA (Applied Biosystems). All PCR reactions were carried out in duplicate and the total RNA input was normalized on the basis of the geometric mean of the Ct values for RNU24 and RNU48 for miRNA. The $2^{-\Delta\Delta Ct}$ method[21] was used to calculate the expression of miR-29a, using the median ΔCT of control samples (for transfection experiments), or the ΔCT of Jurkat T cells (for comparison between T-ALL subgroups). Transcript levels obtained for all T-ALL samples were used in a statistical correlation analysis using a non-parametric Spearman's rank test.

Methylated DNA immunoprecipitation qPCR analysis. Methylation status was determined using the technique of methylated DNA immunoprecipitation (MeDIP) followed by qPCR,[22,23] using a MeDIP kit from Active Motif (Cat. 55009; Carlsbad, CA, USA) according to the manufacturer's instructions. A total of 5 μg genomic DNA in a volume of 300 μL was sonicated on ice with 10 pulses of 30 s (30% amplitude, 130 W, 20 kHz) using a Sonics Vibra-Cell sonicator (VCX 130, Sonics & Materials, Inc., CT, USA) to produce random fragments ranging from 200 to 600 bp. Equal amounts of sonicated DNA from four independent transfections were pooled and two MeDIP experiments were carried. One hundred nanograms of input DNA was diluted 20 × (100 μL final volume) and kept

as a control. One microgram of sheared DNA was submitted to an immunoprecipitation using an antibody that specifically recognizes 5-methylcytidine (5mC) in single-stranded DNA. Briefly, DNA was heated at 95°C for 10 min and immediately transferred to an ice bath. Next, denatured DNA was immunoprecipitated by overnight incubation with antibody (at 4°C) in a final volume of 300 μL of 10 mM Tris-HCL (pH 8.5), with constant gentle rotation and agitation (HulaMixer; Life Technologies, Carlsbad, CA, USA). The DNA was captured with Protein G magnetic beads, washed and eluted to a final volume of 100 μL. The immunoprecipitated DNA (IP) and the input DNA were assayed by qPCR on an CFX96 real-time PCR system (Bio-Rad), using SYBR Green, under the following cycling conditions: 2 min at 50°C, 95°C for 10 min, followed by 40 cycles of 95°C for 25 s and 60 s of annealing, extension at 60–63°C, and a final step of real-time melt analysis to verify product specificity.

Among selected regions, we included genes previously reported as methylated (*GFPT2*, *GNA14*, *SALL1*, *AHR*) or unmethylated (*LHX4*) in Jurkat and Molt-4 cells.[24] For each gene, we used the RefSeq NCBI accession number to search and extract a sequence from −100 to +100 bp around the transcription start site, using the standard search tool from the Eukaryotic Promoter Database (http://epd.vital-it.ch). These regions (all inside a CpG island) were used as templates to design qPCR primers using the PrimerQuest online tool (Integrated DNA Technologies). Additionally, we designed qPCR primers for positive control regions (H19ICR, BRDT, and TSH2B) and negative control regions (HIST1H3B and UBE2B), known as methylated or unmethylated in normal somatic cells, respectively.[22,23] Primer sequences and cycling details for MeDIP qPCR analysis can be found in Table S2.

For each gene, the enrichment of the IP sample relative to the Input sample was calculated by the following equation:

$$2^{\wedge}[(\text{Input CT} - 2.99) - \text{IPCT}]100 \quad (1)$$

where InputCT and IPCT are the cycle threshold values obtained for Input and IP DNA samples, respectively, and 2.99 is the correction factor for the dilution (ln20).Finally, the relative enrichment was calculated by dividing the enrichment observed in the region of interest by the enrichment observed for a negative control region with very few CpGs (IG5).

Patients and treatment protocol. This study included leukemic cells derived from peripheral blood or bone marrow (BM) samples from 40 T-ALL diagnosed patients. All samples were sent to the Hematology Laboratory of the Clinical Hospital of Ribeirão Preto, University of São Paulo (São Paulo, Brazil) between May 1997 and April 2008 for reference diagnostics and registered in our leukemia database.[25] The diagnosis was carried out according to classical criteria established by the WHO. Patients were treated according to the HyperCVAD[26] ($n = 6$), BFM-90[27] ($n = 12$), or GBTLI-ALL99[28] ($n = 20$) protocols. The study was approved by the local Ethics Committee and, in accordance with the Declaration of Helsinki, informed consent was obtained from all patients.

Statistical analysis and clinical end-points. The median values of miR-29a, DNMT3a, DNMT3b, and TET1 expression in leukemic samples were used as references to classify T-ALL patients into high and low expression groups. Student's *t*-test and Fisher's exact tests were used to compare differences between the groups. Overall survival (OS) was defined as the time from the initiation of induction therapy to death from any cause; those alive or lost to follow-up were censored at the date last known alive. Disease-free survival (DFS) was defined as the time from complete remission to disease relapse, development of secondary malignancy, or death from any cause, whichever occurred first. Patients who were alive without disease relapse or secondary malignancy were censored at the time last seen alive and disease-free. Statistical analyses were carried out using SPSS Statistics 17.0 (IBM, Somers, NY, USA). All *P*-values were two-sided. The level of significance was set to 5%. Survival curves were generated by the Kaplan–Meier method and the log–rank test was used for comparisons of Kaplan–Meier curves (level of significance set to 5%).

Effect of miR-29a on proliferation and apoptosis of T-ALL cell lines. In order to measure the effect of miR-29a on the number of viable cells, we used a colorimetric assay based on the capacity of mitochondrial dehydrogenase enzymes present in living cells to reduce XTT into a water soluble, orange formazan product.[29] The Cell Proliferation Kit II (Applied Sciences Roche, Penzberg, Germany) was used according to the manufacturer's protocol. Briefly, 1.0×10^4 cells were plated in 96-well translucent plates (Greiner Bio-One, Frickenhausen, Germany) and were transfected with synthetic miR-29a mimics or control miR (PMC). Cells were evaluated 3 or 5 days post-transfection. The wells were washed with PBS (1 ×), and an XTT solution in complete culture medium (0.3 mg/mL) was added to cells. The plates were covered in aluminum foil and incubated for 3 h at 37°C and 5% CO_2. The absorbance was measured in a multi-well spectrophotometer, VersaMax ELISA Microplate Reader (Molecular Devices, Sunnyvale, CA, USA). Two wavelengths were used, the first captured by the formazan salt (450 nm) and the second was a reference absorbance (650 nm). The net absorbance ($A_{450}-A_{650}$) was used to determine the percentage of viable cells relative to controls:

$$\%\text{Cell proliferation} = (\text{Abs treatment}/\text{Abs control}) \times 100 \quad (2)$$

All experiments were carried out with multiple replicates as specified elsewhere.

The effect of miR-29a on apoptosis was evaluated by flow cytometry 2 days post-transfection. Cells were transferred to tubes, washed, and resuspended in 100 μL binding buffer containing annexin V (2 μL FITC; Cat. 556419; BD Pharmigen, San Diego, CA, USA) and propidium iodide (5 μg PI; Cat. P4170; Sigma Aldrich Life Sciences, St. Louis, MO, USA). Cells were acquired (10 000 events) in a FACSCalibur (Becton Dickinson, Franklin Lakes, NJ, USA) and analyzed using FlowJo (Tree Star Inc, Ashland, OR, USA) to determine the percentage of viable (negative for PI and annexin V), apoptotic (annexin V-positive), and necrotic (annexin V-negative and PI-positive) cells.

Impact of miR-29a on sensitivity of T-ALL cell lines to daunorubicin. We carried experiments based on automated quantitative fluorescence microscopy (high content analysis) to evaluate the impact of miR-29a on the sensitivity of T-ALL cell lines to daunorubicin. Briefly, cells were transfected with synthetic miR-29a mimics or control miR in 96-well plates (Greiner Bio-One). Sixty hours later, the cells were treated or not treated with daunorubicin for 72 h before final evaluation. The concentrations used for Jurkat, Molt-4, and CCRF-Cem were 80 nM, 40 nM, and 40 nM, respectively; these results (for Jurkat and Molt-4) corresponded to previously published IC_{50} values, as determined by MTT assay following 72 h of treatment.[30,31] Following treatment, plates were centrifuged

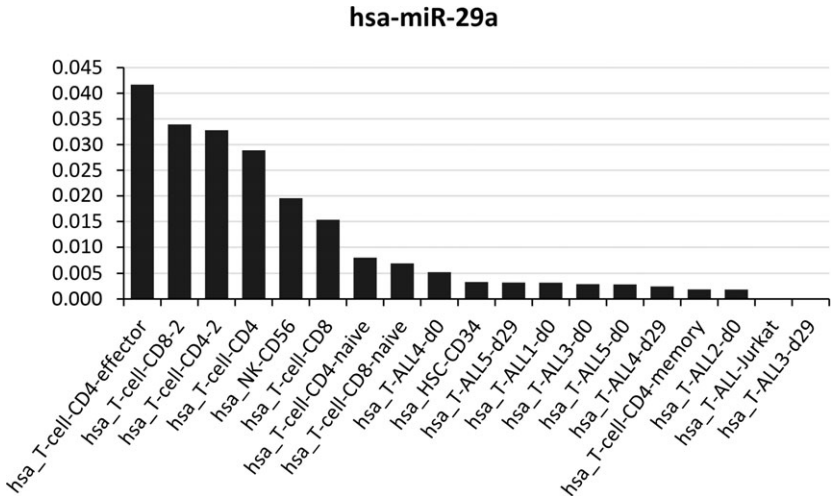

Fig. 1. Expression levels of microRNA-29a (miR-29a) in selected cell types. The expression level of miR-29a is shown for libraries generated from normal T cells, T-cell acute lymphoblastic leukemia (T-ALL) samples, a hematopoietic stem cell $CD34^+$ sample, and the Jurkat cell line (available at microRNA.org). Although not evidenced in the figure, among all the tissues available from microRNA.org, normal T cells are among those with the highest expression levels of miR29a, whereas T-ALL are among those with the lowest levels.

Table 1. Representative miR-29a predicted target transcripts identified by microarray

Transcript ID	Gene	Description	No. of sites
NM_144993	*TET3*	Tet oncogene family member 3 (TET3)	8
NM_015886	*PI15*	Peptidase inhibitor 15 (PI15)	5
NM_000093	*COL5A1*	Collagen, type V, alpha 1 (COL5A1)	4
NM_030625	*TET1*	Tet oncogene 1 (TET1)	4
NM_020443	*NAV1*	Neuron navigator 1 (NAV1), transcript variant 1	4
NM_198686	*RAB15*	RAB15, member RAS onocogene family (RAB15)	3
NM_001259	*CDK6*	Cyclin-dependent kinase 6 (CDK6), transcript variant 1	3
NM_145725	*TRAF3*	TNF receptor-associated factor 3 (TRAF3), transcript variant 1	3
NM_005595	*NFIA*	Nuclear factor I/A (NFIA), transcript variant 2	3
NM_032410	*HOOK3*	Hook homolog 3 (Drosophila) (HOOK3)	3
NM_000501	*ELN*	Elastin (ELN), transcript variant 1	3
NM_001134673	*NFIA*	Nuclear factor I/A (NFIA), transcript variant 1	3
NM_021643	*TRIB2*	Tribbles homolog 2 (Drosophila) (TRIB2), transcript variant 1	3
NM_173566	*PRR14L*	Proline rich 14-like (PRR14L)	3
NM_017552	*ATAD2B*	Atpase family, AAA domain containing 2B (ATAD2B), transcript variant 1	3
NM_001099270	*ZBTB34*	Zinc finger and BTB domain containing 34 (ZBTB34)	3
NM_173595	*ANKRD52*	Ankyrin repeat domain 52 (ANKRD52)	3

(170 *g*, 5 min), media were removed and cells were washed once with binding buffer (0.1 M HEPES, 1.4 M NaCl, and 25 mM CaCl2, pH 7.4). Next, cells were incubated with 50 μL binding buffer containing the nuclear stain Hoechst 33342 (3 μg/mL), annexin V (15 μL/mL, Alexa Fluor 488; Cat. A13201; Life Technologies) and PI (1.5 μg/mL; Cat. P4170; Sigma Aldrich Life Sciences). Finally, images were acquired using an ImageXpress^{MICRO} XLS high-content imaging system and submitted to image segmentation and scoring using the Cell Health Module of the MetaXpress software (Molecular Devices).

Results

MicroRNA-29a expression in normal and leukemic T cells. Our database survey showed that, among all libraries available at microRNA.org (including all types of normal or neoplastic cells or tissues), those derived from normal T lymphocytes were the ones who presented the highest levels of miR-29a expression. Strikingly, T-ALL samples presented the lower levels of miR-29a expression (comparable to normal $CD34^+$ HSC). In agreement, the leukemic T cell line (Jurkat) had one of the lowest levels of this specific miRNA (Fig. 1, Table S3). These findings suggest that reduced miR-29a expression might be related with the pathophysiology of T-ALL. Based on this observation, we used a large-scale approach in order to identify potential miR-29a target transcripts in T-ALL.

Microarray identification of miR-29a targets. When comparing the set of 1078 genes coding for miR-29a predicted targets (obtained from TargetScan) to the set of transcripts identified by our microarray analysis (downmodulated in the Jurkat cell line following introduction of miR-29a mimics), we identified 543 targets (considered to be subjected to miR-29a-induced degradation) displaying a total of 649 target sites for miR-29a (Table S4). By totaling the number of miR-29a target sites in each of these transcripts, and ordering transcripts by this total, we found that transcripts such as TET3 and TET1 were among those with the highest number of sites, with a total of nine and four sites, respectively (Tables 1,S5). In addition to TET1 and TET3, thymine DNA glycosylase (TDG) was also identified as a target. Interestingly, all of these transcripts code for proteins involved in the process of active demethylation. Importantly, established miR-29 targets, such as DNMT3a, DNMT3b,

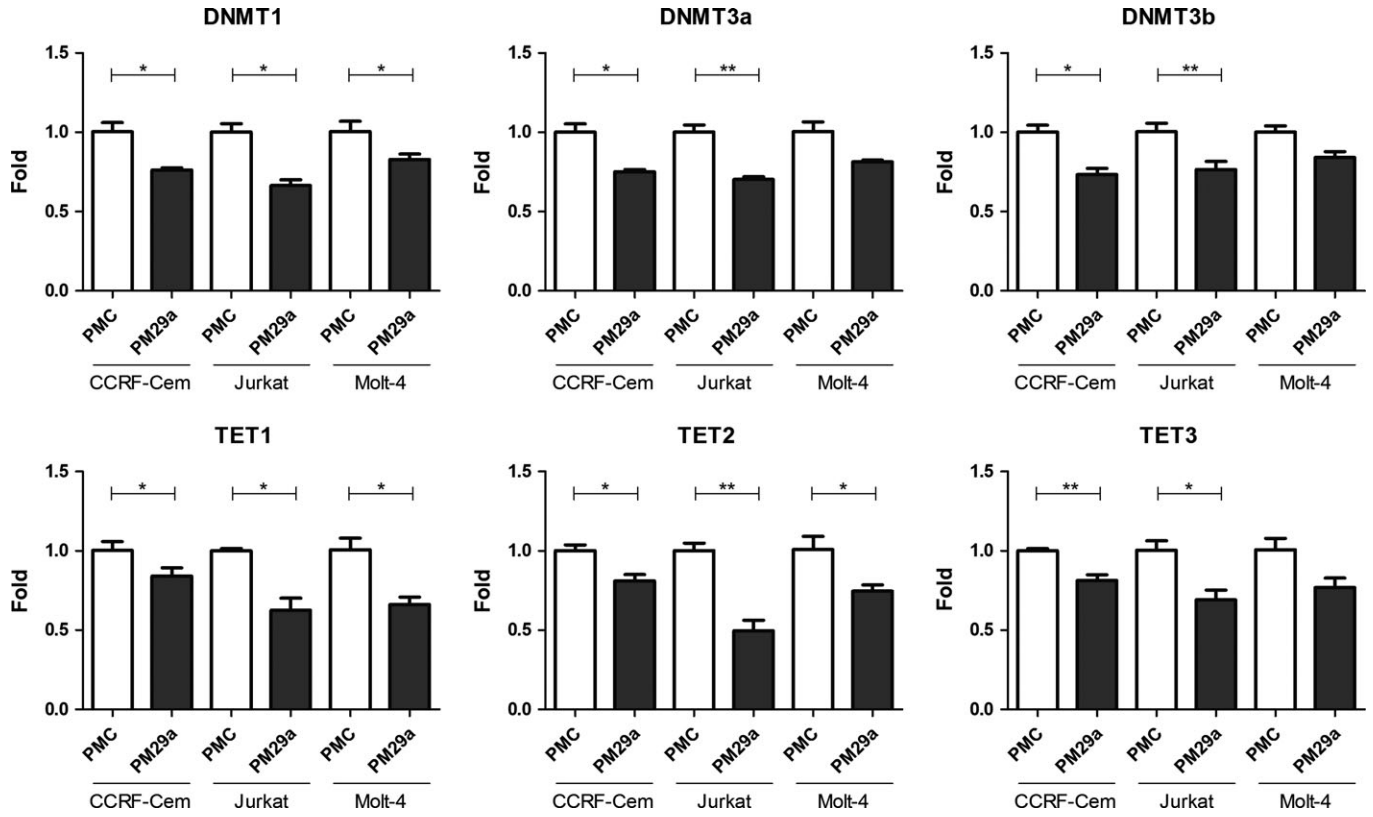

Fig. 2. Effect of microRNA-29a (miR-29a) on transcript levels of selected targets. The T-cell acute lymphoblastic leukemia cell lines Jurkat, Molt-4, and CCRF-Cem were transfected with miR-29a synthetic mimics (PM29a) and a corresponding control unspecific miR molecule (PMC) and transcript levels of selected targets (TET1, TET2, TET3, DNMT1, DNMT3A, and DMNT3B) were evaluated by real-time quantitative PCR after 48 h. Significantly lower transcript levels were observed in cells transfected with miR-29a (non-paired *t*-test, two-tailed). $*P < 0.05$; $**P < 0.01$.

CDK6, and PXDN were also identified by us, corroborating our experimental approach.

Functional analysis of miR-29a targets. Functional analysis using the set of 531 transcripts led to the identification of several pathways (VEGF, WNT, Jak/Stat signaling) that were statistically enriched with the potential miR-29a targets (Table S6), including the following genes: *COL4A1*, *PDGFB*, *IGF1*, *CDK6*, *MAPK10*, *FZD4*, *ITGB1*, *PTEN*, *ARNT*, *TGFB2*, *LAMA2*, *FOS*, *NRAS*, *ITGA6*, *VEGFA*, *RARB*, *PIK3R3*, *PIK3R1*, *TRAF4*, *AKT3*, and *TRAF3*.

Validation of selected target transcripts. As compared to cells transfected with unspecific control miRs, the transcript levels of all selected targets evaluated by real time qPCR (TET1, TET2, TET3, DNMT1, DNMT3A, and DMNT3B) were reduced following 48 h of transfection with the miR-29a mimics. This was statistically significant ($P < 0.05$, $n = 4$) for all T-ALL cell lines (Jurkat, Molt-4, and CCRF-Cem), except for DNMT3A, DMNT3B, and TET3 in Molt-4 cells (Fig. 2).

The Jurkat cells used for the microarray experiments were also evaluated by qPCR. The introduction of miR-29a was confirmed (Fig. S1). Accordingly, the transcript levels of the evaluated genes were reduced, although the reduction was found to be significant ($P < 0.05$, $n = 3$) only for TET1, TET3, and DMNT3b (Fig. S2).

MicroRNA-29a target regulation in T-ALL patients. In order to investigate whether the expression of the validated targets could be under the control of miR-29a in leukemic cells derived from T-ALL patients, we evaluated the expression levels of miR-29a and of DNMT3a, DNMT3b, and TET1 by real-time PCR, and undertook a correlation analysis. We observed an inverse correlation between miR-29a and the transcripts evaluated (Fig. 3), suggesting that miR-29a could be involved in the *in vivo* regulation of the identified targets in primary T-ALL cells.

Effect of miR-29a on promoter demethylation and transcriptional modulation. Real-time qPCR of methylated DNA immunoprecipitates (obtained by MeDIP) allowed us to access the enrichment (i.e. relative methylation status) of selected regions (Fig. 4a). As expected, the negative control regions HIST1H3B and UBE2B (unmethylated in normal somatic cells) showed a very small enrichment in both T-ALL cell lines (all below 7-fold). Similarly, the region from the *LHX4* gene, reported by Kuang *et al.* as a region with low-level methylation in Jurkat and Molt-4 cells (5.4% and 4.3%, respectively, bisulfite pyrosequencing),[24] had a very low enrichment (approximately 14- and 7-fold, respectively). Furthermore, the positive control regions TSH2B and H19ICR (methylated in normal somatic cells) were also highly enriched in Jurkat cells (62- and 26-fold, respectively); however, in Molt-4 cells, whereas TSH2B was also enriched (33-fold), H19ICR had a very low enrichment level (4-fold). Finally, enrichment of the BRDT region was very low in both cell lines (<4-fold), differing from normal somatic cells.

Completely in line with the results of Kuang *et al.*,[24] the SALL1, GNA14, and GFPT2 regions were all highly enriched in Jurkat and Molt-4 cells (412-, 207-, and 103-fold and 95-, 79-, and 22-fold, respectively). Moreover, the relative enrichment observed by us was well correlated with the percentage

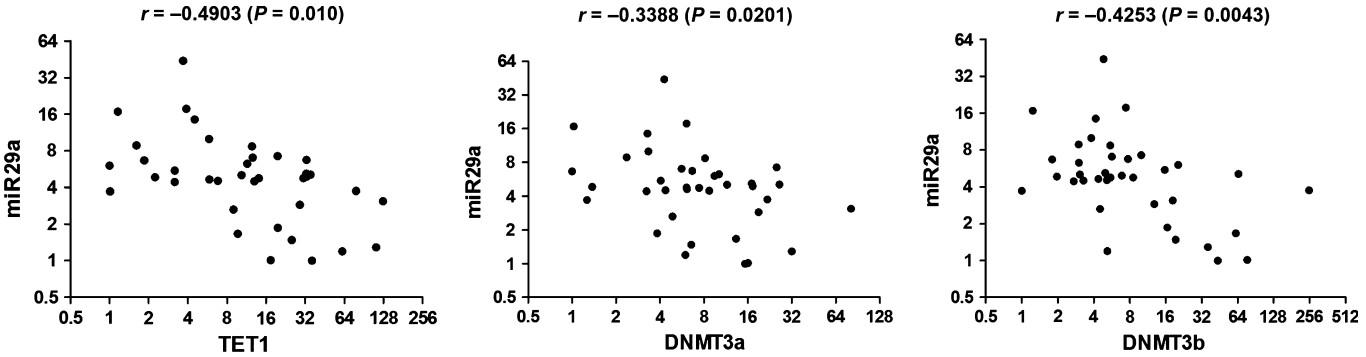

Fig. 3. Correlation analysis between microRNA-29a (miR-29a) and selected target transcripts in T-cell acute lymphoblastic leukemia samples. Transcript levels of TET1, DNMT3A, DMNT3B and miR-29a were evaluated by real-time quantitative PCR in the leukemia samples and a correlation analysis was carried. A statistical significant inverse correlation (negative *r* value, Pearson's correlation coefficient) was observed between the levels of miR-29a and all transcript targets evaluated ($n = 37$).

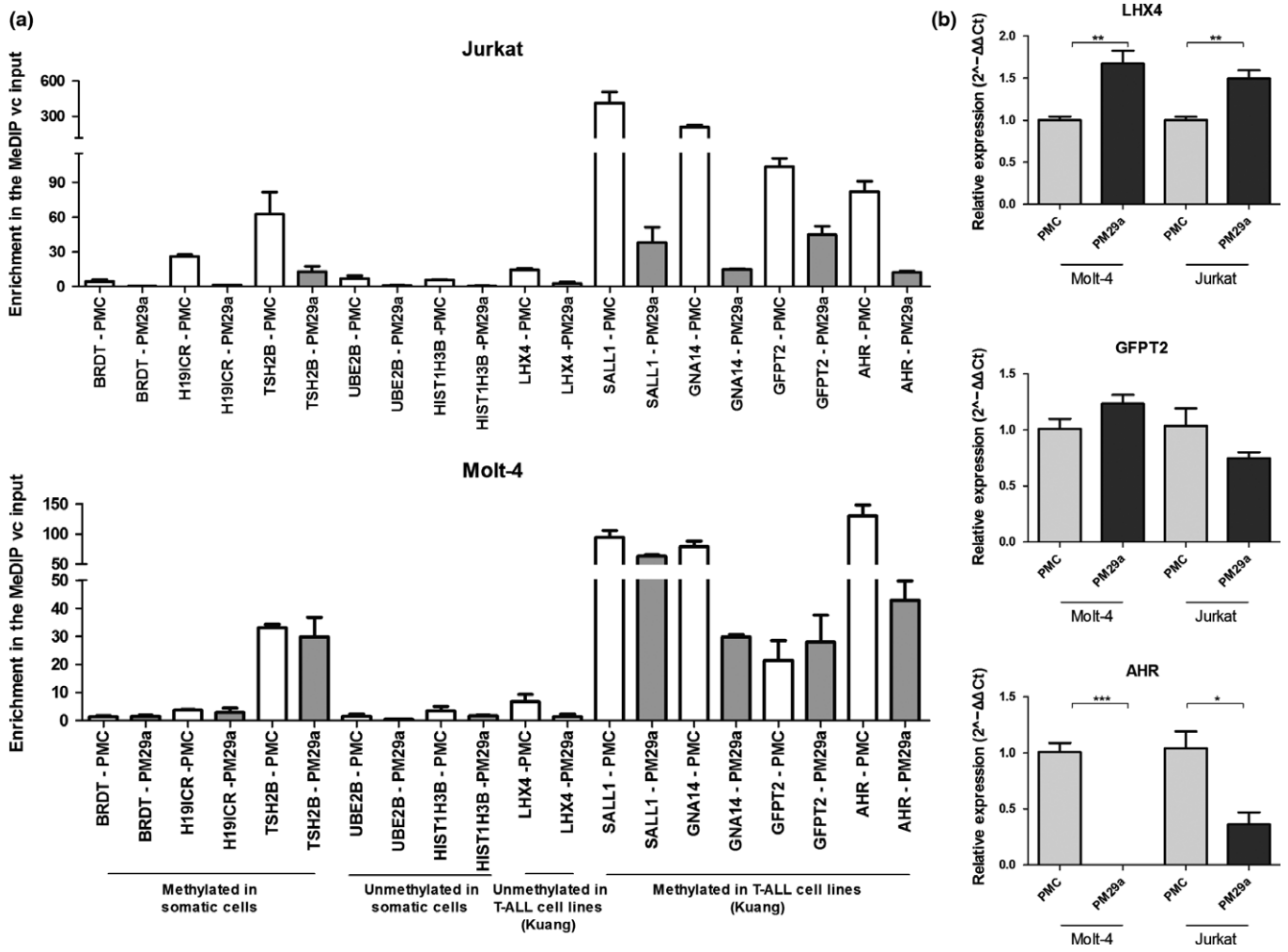

Fig. 4. Effect of microRNA-29a (miR-29a) on promoter methylation and expression of selected genes. The T-cell acute lymphoblastic leukemia (T-ALL) cell lines Jurkat and Molt-4 were transfected with miR-29a synthetic mimics (PM29a) and a corresponding control unspecific miR molecule (PMC) and, 48 h later, DNA and RNA was collected and evaluated. (a) Methylation status was evaluated by immunoprecipitation of methylated DNA (meDIP) followed by quantitative PCR (using primers directed to a CpG island region encompassing the transcription start site). For each gene, the enrichment was calculated by initially normalizing the CT values of the immunoprecipitated DNA sample by the CT values of the Input DNA sample, then calculating the enrichment relative to the enrichment observed for a negative control region (a region with very few CpGs from the *IG5* gene). Selected genes, included those previously reported by Kuang *et al.*[24] as methylated in Jurkat and Molt-4 cells (including *GFPT2*, *GNA14*, *SALL1*), positive control regions from *H19ICR*, *BRDT*, and *TSH2B* genes (methylated in normal somatic cells), and negative control regions from *HIST1H3B* and *UBE2B* genes (unmethylated in normal somatic cells) and from the *LHX4* gene (reported by Kuang *et al.* as unmethylated in Jurkat and Molt-4 cells). Results are the mean of two meDIP experiments carried out with a pool of four independently transfected samples. (b) Transcript levels of selected targets were evaluated by real-time quantitative PCR. Statistical significance was evaluated by a two-tailed non-paired *t*-test ($n = 4$). $^*P < 0.05$; $^{**}P < 0.01$; $^{***}P < 0.001$.

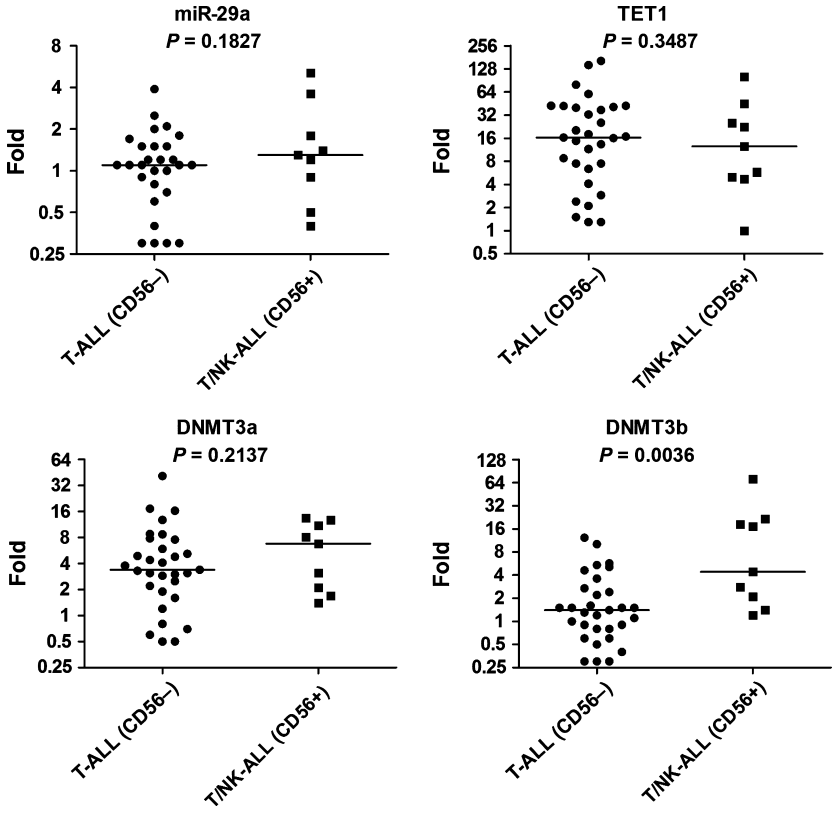

Fig. 5. Gene expression of microRNA-29a (miR-29a) target in T-cell acute lymphoblastic leukemia T-ALL subgroups. The comparison between T-ALL patients ($CD56^-$) (n = 31) with the specific subtype T/NK-ALL ($CD56^+$) (n = 9) by quantitative RT-PCR revealed significantly higher levels of DNMT3b in the latter group; there were no significant differences in TET1 or DNMT3a (one-tailed Mann–Whitney test).

of methylation obtained by Kuang *et al.*[24] (88, 89, and 90% and 75, 68, and 13%, respectively). Strikingly, transfection of miR-29a led to demethylation of the promoter region of *GNA14*, *SALL1*, *AHR*, and *LHX4* genes, in Jurkat and Molt-4 cells, whereas *GFPT2* was demethylated only in Jurkat cells. Of note, transfection of miR-29a also led to demethylation of the TSH2B and H19ICR regions in Jurkat cells. These results were in line with a preliminary experiment evaluating the *AHR* gene by MS-PCR using bisulfite-treated DNA from Jurkat cells electroporated with miR-29a or a control miR (Fig. S3). Overall, these results indicate that reduced methylation resulting from miR-29a introduction may be a broadly acting mechanism, likely mediated by targeting of DNMTs.

Real-time qPCR evaluation of the corresponding transcripts revealed that, while the expression of *LHX4* was significantly induced, that of *AHR* was significantly repressed in Jurkat and Molt-4 cells transfected with miR-29a, as compared to control cells. Finally, *GFPT2* expression levels did not vary significantly (showing opposite trends in both cell lines) and *SALL1* was not detected in either Jurkat or Molt-4 cells (Fig. 4b).

T/NK-ALL patients have significantly higher DNMT3b levels. The comparison between the levels of miR-29a and its targets, observed in $CD56^-$ T-ALL patients and the subgroup of $CD56^+$ T/NK-ALL (T-cell/natural-killer acute lymphoid leukemia) patients and previously shown to be associated with worse response to treatment,[25] revealed significantly higher levels of DNMT3b in the T/NK-ALL group, but no differences in expression of miR-29a or the remaining transcripts evaluated (Fig. 5).

Clinical outcome according to miR-29a expression. The main clinical and laboratory features of enrolled patients are summarized in Table 2. There was no relevant difference between T-ALL patients with low and high mir-29a expression with respect to clinical and laboratory features (Table 2), except for the percent of BM blast and platelets counts, which were higher ($P = 0.022$) and lower ($P = 0.02$), respectively, in patients with low mir-29a expression. Regarding DNMT3a, DNMT3b, and TET1 expression levels and clinical and laboratory features, no relevant differences were detected between groups (Table S7).

The mean follow-up of our patients was 27 months (range, 12–42 months) and the estimated 5-year OS rate was 36%. The complete remission rate for the whole population was 66% and did not differ between low- and high-miR-29a (70% *versus* 66%; $P = 0.825$). High miR-29a patients had a significantly lower DFS (54%) compared with low miR-29a patients (91%) ($P = 0.027$; Fig. 6a). However, the differences in OS observed between patients expressing high or low miR-29a levels did not reach statistical significance (49% *vs.* 30% in low- *vs.* high-miR374 groups, respectively; $P = 0.169$; Fig. 6b). *DNMT3a* (DFS, $P = 0.265$; OS, $P = 0.774$), *DNMT3b* (DFS, $P = 0.151$; OS, $P = 0.842$), and *TET1* (DFS, $P = 0.315$; OS, $P = 0.319$) gene expression was not associated with treatment outcome in T-ALL (Table S7, Fig. S4).

Effect of miR-29a on proliferation and apoptosis of T-ALL cell lines. Evaluation of cell viability by XTT assay on Jurkat and Molt-4 T-ALL cell lines 3 and 5 days post-transfection revealed that, compared to reference cells transfected with a control miR, miR-29a had no statistically significant impact, however, a slight increase on proliferation was observed for Jurkat and Molt-4 cells 5 days post-transfection (Fig. 7a). Flow cytometry evaluation of apoptosis in Jurkat and Molt-4 cells revealed no significant differences 2 days post-transfection (Fig. 7b–d).

Impact of miR-29a on sensitivity of T-ALL cell lines to daunorubicin. Automated quantitative fluorescence microscopy analysis of Jurkat, Molt-4, and CCRF-Cem cells revealed no significant impact of miR-29a on the total number or percentage of viable

Table 2. Clinical features of T-ALL patients at diagnosis according to expression of miR-29a

Patient Characteristics	miR-29a				*P*-value†
	Low expression (n = 19)		High expression (n = 18)		
	No.	%	No.	%	
Age‡, years	18		20.6		0.58
Range	1–53		3–58		
Gender (M/F)					0.867
Male	15	78.9	14	77.8	
Female	4	21.1	4	22.2	
Mediastinal mass (%)					0.184
Absent	8	57.1	3	27.3	
Present	6	42.9	8	72.7	
Missing	5	–	7	–	
Lymphadenopathy (%)					0.289
Absent	6	35.3	3	17.6	
Present	11	64.7	14	82.4	
Missing	2	–	1	–	
Splenomegaly (%)					0.216
Absent	1	6.7	3	23.1	
Present	14	93.3	10	76.9	
Missing	4	–	5	–	
Hepatomegaly (%)					0.502
Absent	2	13.3	3	23.1	
Present	13	86.7	10	76.9	
Missing	4	–	5	–	
CNS involvement (%)					0.854
Absent	11	84.6	7	87.5	
Present	2	15.4	1	12.5	
Missing	6	–	10	–	
Hemoglobin‡ (g/L)	9.45		11.6		0.055
Range	4.6–15.8		3.6–15.6		
WBC‡ count $\times 10^9$/L	20.3		86.8		0.59
Range	4.5–789		4.6–236		
Platelets‡ $\times 10^9$/L	59.8		142.5		0.02*
Range	9–299		9–474		
Blasts BM‡ (%)	91.9		71		0.022*
Range	28–100		21–100		
Blasts PB‡ (%)	77.7		61		0.225
Range	10–100		1–100		

CNS, central nervous system; WBC, white blood cell; PB, peripheral blood; BM: bone marrow. †Missing values were excluded in the calculation of *P*-values. ‡Values represent mean (range). *Statistically significant differences.

cells (Fig. 8a,b). As expected, 72 h of treatment of Jurkat and Molt-4 cells with previously stablished IC_{50} concentrations of daunorubicin resulted in percentages of viable cells around 50% (approximately 40 and 60%, respectively) for cells transfected with control miR (Fig. 8b). In some instances, miR-29a promoted a statistically significant increase in the percentage of apoptotic cells, accompanied by a decrease in the percentage of non-apoptotic necrotic cells (Fig. 8c,d).

Discussion

The miR-29 family members have been implicated in leukemogenesis; however, their role is not well established.[5–9] Here, we showed that miR-29a levels was reduced in T-ALL and the Jurkat T cell line compared to normal T cells, a key feature that could be linked to the accumulation of oncogenic targets, potentially involved in the molecular pathophysiology of T-ALL. By carrying out a microarray analysis in the Jurkat cell line transfected with synthetic miR-29a mimics, we observed the downregulation of several predicted targets, and thus, presumably true miR-29a targets in T-ALL. Importantly, our analysis allowed the identification of previously identified miR-29 targets, including *DNMT3a* and *DNMT3b*,[32] *CDK6*,[6,12] *PXDN*,[33] *MCL1*,[6,34,35] the *p53* upstream inhibitors *p85a* (or *PIK3R1*),[36] as well as *CXXC6*.[37,38] These results largely corroborate our experimental approach and further indicate that targets implicated in other types of cancers may also play a critical role in T-ALL.

Our functional analysis led to the identification of pathways with described roles in distinct cancer types previously associated with reduced miR-29 expression levels. For instance, we found enrichment for transcript targets associated with non-small-cell lung cancer (NSCLC)[5,39] and melanoma.[40] Moreover, cancer types that were previously shown to be associated with increased miR-29 expression levels, such as colon, pancreas, and prostate cancers,[5] were also identified by our functional analysis (Table S6).

In addition to the direct targeting of transcripts coding for oncogenes such as *MCL1*, *CDK6*, and *PIK3R1*[6,12,34–36] or tumor suppressors such as *PXDN*,[33] the mir-29 family can act indirectly, through epigenetic mechanisms intermediated by the targeting of transcripts coding for the DNA methyltransferases DNMT3a or DNMT3b.[32]

Epigenetic regulation involves DNA methylation at the 5-position of cytosine in CpG dyads (generating 5mC), which is established and maintained by DNA methyltransferases (DNMT1, DNMT3A, and DNMT3B). DNMT1 has a substrate preference for hemimethylated DNA, maintaining methylation patterns during replication,[41] whereas DNMT3A/B methylates DNA *de novo*, irrespective of any methylation.[42,43] As a result, while reduced levels of DNMTs can lead to passive demethylation, due to successive DNA replications cycles, increased levels may lead to hypermethylation.[44]

In fact, in NSCLC, the reduced levels of miR-29 family members[5,39] are responsible for the increased methylation of tumor suppressor genes, and forced expression of miR-29 in lung cancer cell lines leads to their demethylation and consequent re-expression, inhibiting tumorigenicity.[32]

Similarly, miR-29 is found at reduced levels in samples from newly diagnosed AML patients (as compared to $CD34^+$ cells from healthy donors)[45] and in pediatric AML patients with poor prognosis.[46] In addition, forced expression of miR-29b induces global DNA hypomethylation and tumor suppressor gene re-expression in AML cell lines, by targeting directly DNMT3A/B and indirectly DNMT1.[38,47] In apparent contrast to the above results, the ectopic expression of miR-29a in mouse HSCs promotes self-renewal of myeloid progenitors, leading to a myeloproliferative disorder and, ultimately, to AML.[14]

Interestingly, our approach allowed the identification of several targets that may help to elucidate such contrasting effects. Among these targets, we were surprised to identify transcripts coding for members of the TET family and TDG, proteins whose roles in epigenetic regulation (more specifically in active DNA demethylation), have only begun to be envisioned.[44] Of note, we found that TET1 was previously identified as a miR-29 target, but under the alias CXXC6,[6,37] probably leading the authors to overlook the important epigenetic function of this protein.

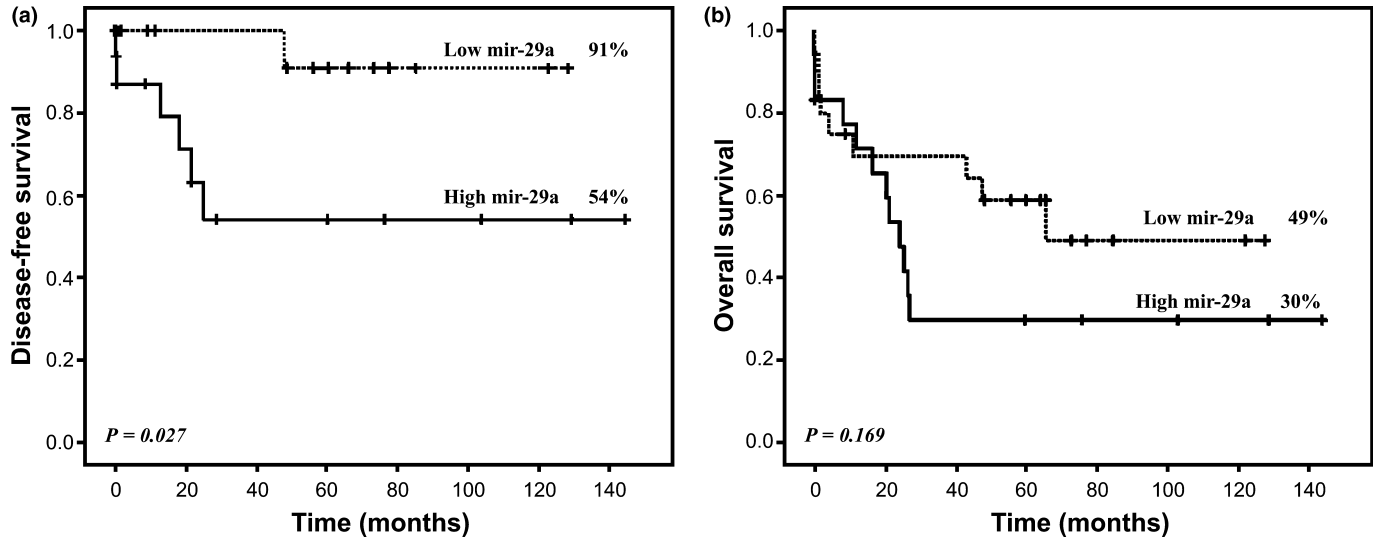

Fig. 6. Disease-free survival (a) and overall survival (b) in T-cell acute lymphoblastic leukemia patients according to microRNA-29a (miR-29a) expression. Survival curves were generated by the Kaplan–Meier method and the log–rank test was used for comparisons of Kaplan–Meier curves (level of significance set to 5%).

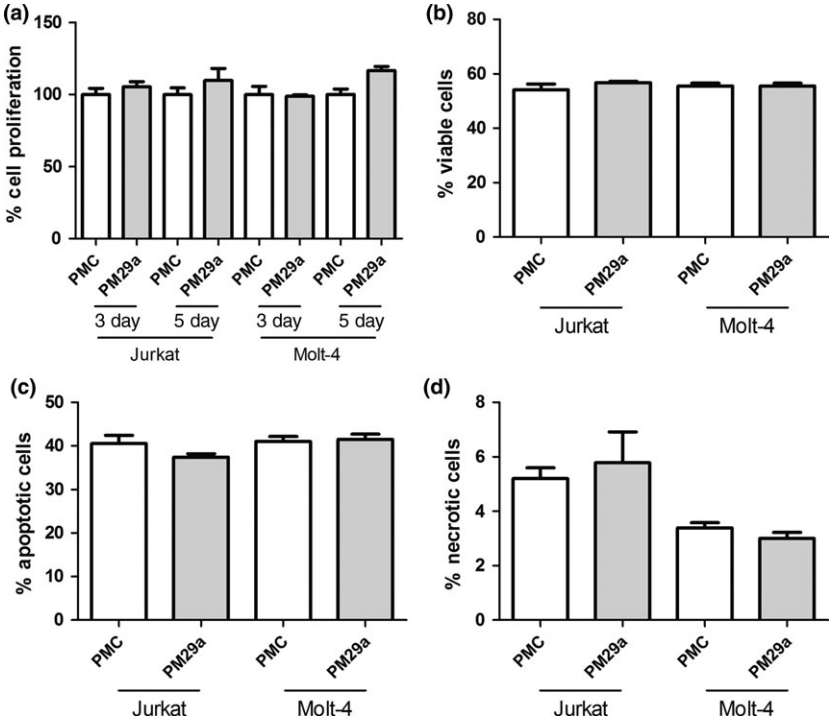

Fig. 7. Effect of microRNA-29a (miR-29a) on proliferation and apoptosis of T-cell acute lymphoblastic leukemia cell lines. The cell lines Jurkat and Molt-4 were transfected with miR-29a synthetic mimics (PM29a) and a corresponding control unspecific miR molecule (PMC). (a) Percentage of viable cells, relative to controls, determined by XTT assay 2 and 5 days (d) post-transfection. (b–d) Flow cytometry analysis, 2 days post-transfection, of viable (negative for propidium iodide and annexin V), apoptotic (annexin V-positive), and necrotic (annexin V-negative and propidium iodide-positive) cells. No significant differences were observed (one-way ANOVA with Bonferroni's multiple comparison test).

In mammals, 5mC can be hydroxylated by the TET family of dioxygenases to generate 5hmC. 5hmC is poorly recognized by DNMT1, leading to replication-dependent passive demethylation. It can be further oxidized by TET proteins to produce 5fC and 5caC. Alternatively, 5hmC may be further deaminated by AID/APOBECC deaminases to become 5hmU. In turn, 5hmU, 5fC, and 5caC can be excised from DNA by glycosylases such as TDG.[48]

The *TET* family of genes (*TET1*, *TET2*, and *TET3*) have been implicated as tumor suppressors in hematological malignancies, initially with the identification of TET1 as a partner of *MLL* in rare chromosomal translocations[49] and, later, by the demonstration of acquired mutations targeting *TET2* in various myeloid disorders, including AML.[50] Moreover, mice with conditional TET2 haploinsufficiency in the hematopoietic compartment displayed increased stem cell self-renewal, extramedullary hematopoiesis, and eventual myeloproliferation, suggesting a contribution to hematopoietic transformation.[51] Based on the above findings, it is tempting to propose that one of the mechanisms by which forced expression of miR-29 in hematopoietic progenitors may lead to AML, would be by direct downregulation of the miR-29 targets, *TDG* and *TET* family members, identified by us.

Although the roles of miR-29 family members in AML have been more thoroughly studied, their roles in T-ALL are still largely unexplored. Given our observations that miR-29a levels

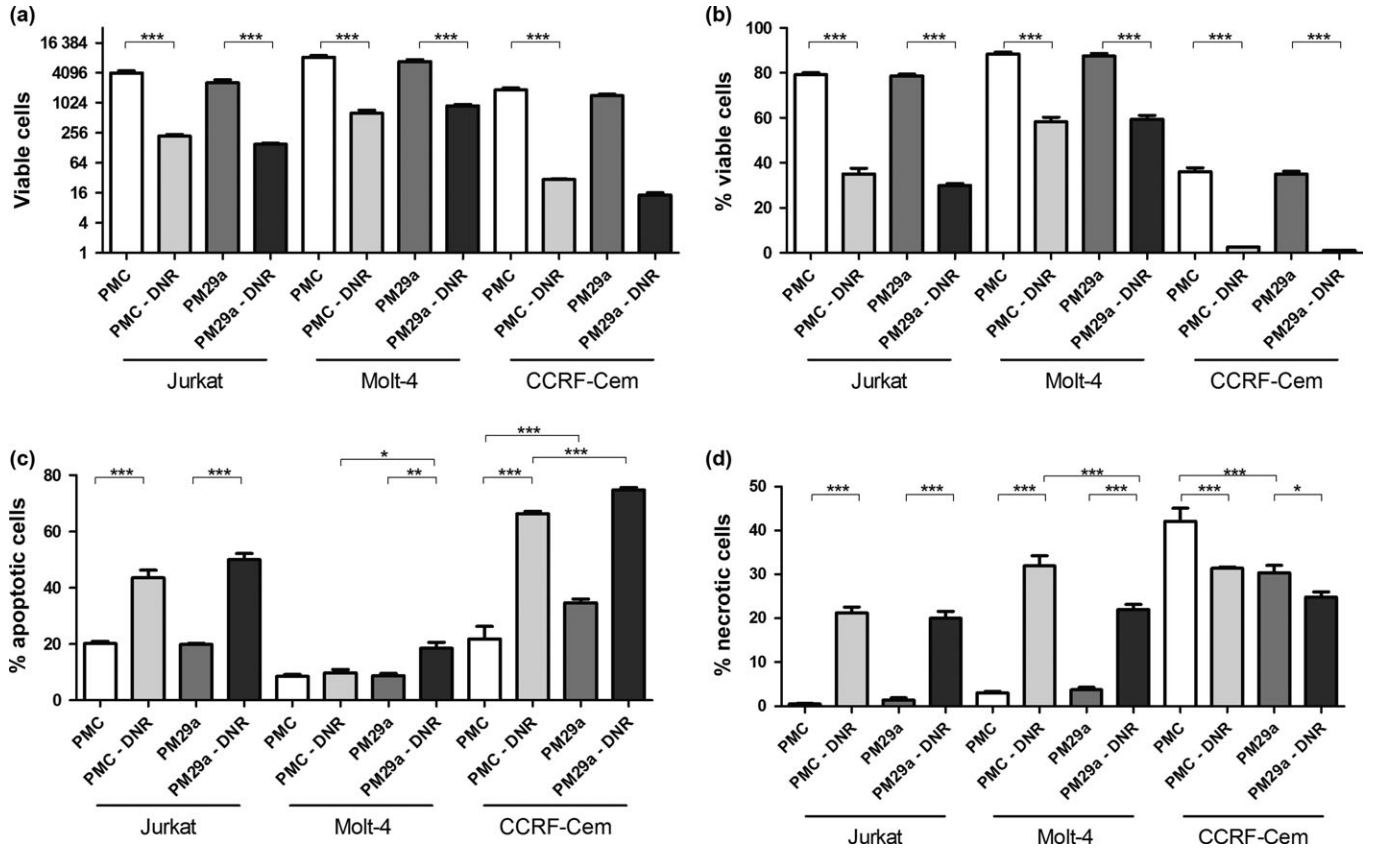

Fig. 8. Impact of microRNA-29a (miR-29a) on the sensitivity of T-cell acute lymphoblastic leukemia cell lines to daunorubicin. The cell lines Jurkat, Molt-4, and CCRF-Cem were transfected with miR-29a (PM29a) synthetic mimics and a corresponding control unspecific miR molecule (PMC). Following 60 h of transfection, cells were treated with daunorubicin (DNR) (80 nM, 40 nM, and 40 nM, respectively) for 72 h and evaluated by automated quantitative fluorescence microscopy analysis. (a) Total number of viable cells (negative for propidium iodide [PI] and annexin V). (b–d) Percentage of viable (negative for PI and annexin V), apoptotic (annexin V-positive), and necrotic (annexin V-negative and PI-positive) cells. There were no significant differences in the number or percentage of viable cells, however, in some instances, miR-29 promoted a significant increase in the percentage of apoptotic cells, accompanied by a decrease in the percentage of non-apoptotic necrotic cells (one-way ANOVA with Bonferroni's multiple comparison test). *P < 0.05; **P < 0.01; ***P < 0.001.

are reduced in T-ALL samples and in the Jurkat lineage (compared to normal T cells), based on the targets identified by us, we sought to explore whether targeting of DNMTs by restored miR-29a levels in Jurkat cells would impact the epigenetic machinery, as previously shown for NSCLC[32] and AML cell lines.[38,47]

Based on the identified targets, miR-29a could lead to decreased methylation (by targeting DNMTs), or to increased methylation (by targeting TETs and TDG). To evaluate this, we initially accessed the effect of introducing miR-29a into Jurkat cells in the methylation status of the promoter region of the *AHR* gene, known to be commonly methylated in ALL,[52,53] by MS-PCR. AHR is a ligand-activated transcription factor that was proposed to contribute to cell cycle control through interaction with retinoblastoma protein.[54] In line with this proposal, activation of AHR led to growth inhibition of pancreatic[55] and prostate[56] cancer cells. Nonetheless, its roles in cell proliferation are controversial. Transient expression of a constitutively active form of AHR in Jurkat T cells, induce growth arrest.[57] In contrast, in T-ALL cell lines and in some primary adult T-ALL cells, AHR was found to be constitutively activated in the absence of apparent exogenous ligands, establishing a link with leukemogenesis.[58] Moreover, while downregulation of AHR (by siRNA) leads to an increase in the proliferation of the HepG2 liver cell line, it decreases the growth of the MCF-7 breast tumor cell line.[59] This further indicates that the cellular context can greatly impact the functional outcomes of a given miR, not only through alternative targets, but also through alternative context-dependent roles of its targets.

In ALL, the transcription of the *AHR* gene is silenced by promoter hypermethylation, through inhibition of Sp1 binding.[53] Importantly, we showed that introduction of miR-29a mimics in Jurkat cells leads to the demethylation of the AHR promoter, which would be probably mediated by the direct targeting of DNMT3a and DNMT3b. Nevertheless, given that miR-29 has been shown to indirectly downregulate DNMT1, by directly targeting its transactivator Sp1,[38,47] the expected effect of miR-29a in the transcription of the *AHR* gene would not be straightforward to predict.

In order to more widely access the roles of miR-29a in T-ALL's epigenetic landscape, we extended our methylation analysis to additional genes, including: *LHX4*, *GFPT2*, and *SALL1*. Our selection was based on the methylation pattern observed by Kuang *et al.* (using pyrosequencing) in several cell lines (including the T-ALL cell lines Jurkat and Molt-4), peripheral blood cells from T-ALL patients and healthy controls.[24]

To this end, we used MeDIP followed by qPCR[22,23] in Jurkat and Molt-4 cells. Strikingly, in addition to corroborating

the MS-PCR results obtained for AHR, MeDIP analysis revealed that transfection of miR-29a led to demethylation of several additional regions, including the CpG islands in the promoters of *GNA14*, *SALL1*, and *LHX4* genes in Jurkat and Molt-4 cells, and of *GFPT2*, *TSH2B*, and *H19ICR*, in Jurkat cells.

Real-time qPCR evaluation of the transcript levels of the evaluated genes revealed that their behavior could not be predicted solely by the demethylation status. For instance, while miR-29a transfection led to demethylation of the *AHR* gene in Jurkat and Molt-4 cell lines, its expression was decreased, likely by the direct targeting of Sp1 by miR-29a.[53] Moreover, the expression of *LHX4* was significantly induced in Jurkat and Molt-4 cells transfected with miR-29a, compared to control cells, whereas *GFPT2* expression levels did not vary significantly, and actually showed opposite trends in both cell lines. While introduction of miR-29a can rapidly lead to reduced protein levels of its targets (by mRNA destabilization /cleavage or translational inhibition), its secondary (demethylation of promoter CpG islands) and tertiary effects (transcriptional modulation) occur later on. Thus, although the time period of 48 h allowed us to clearly see the epigenetic effect of miR-29a, it may have not been sufficient to allow the transcription of the corresponding genes.

Given the complex and controversial roles of miR-29a and its targets, in leukemia and cancer, we evaluated the potential association of their expression levels in a previously studied T-ALL patient cohort.[25,60] While we could identify significantly higher levels of DNMT3b in the T/NK-ALL group (previously associated with worse response to treatment), no difference was observed for the expression of miR-29a. Although these results do not indicate the regulation of DNMT3b levels by miR-29a in these patients, the identification of a significant inverse correlation between miR-29a and DNMT3b (as well as DNMT3a and TET1), indicates that these transcripts may be under the control of miR-29a or, more generally, under the composite control of distinct miR-29 family members. Noteworthy, the miR-29 family comprises three variants, and miR-29b-1 and miR-29a are located in the same cluster on chromosome 7q32 and are, thus, co-expressed; miR-29b-2 and miR-29c are located on chromosome 1q23.[61]

When we independently evaluated the potential association of miR-29a and selected transcript targets with DFS or OS, we found that higher expression levels of miR-29a were significantly associated with worse DFS, in apparent contrast with the finding for CLL and AML.[12,14,33] Interestingly, the percentage of BM blasts was significantly higher in patients with low miR-29a levels, which could potentially indicate increased proliferation in the leukemic cells expressing lower levels of miR-29a. These apparently contrasting findings could be conciliated by the increased efficiency of chemotherapeutic agents in the more proliferative leukemic blasts (expressing lower miR-29a levels) during induction therapy. This would be in line with the recent finding that reduced miR29 expression in HSC increases cell cycling but also increases apoptosis, an effect that would be mediated by increased levels of DNMTs.[62] Our results, however, did not show a significant impact of miR-29a in the proliferation or viability of T-ALL cell lines. Actually, a slight increase on proliferation was observed for Jurkat and Molt-4 cells at 5 days post-transfection with miR-29a. Moreover, at this time point, miR-29a apparently promoted a change in the mechanism of cell death, with an increased percentage of apoptotic cells, paralleled by a decreased percentage of non-apoptotic necrotic cells. Despite these results, the transient effect mediated by the introduction of a synthetic miR-29a mimic cannot recapitulate the long-term effect of a continuous higher expression. As a matter of fact, following the direct primary effects of miR-29a, a myriad of indirect effects are expected to occur (e.g. by targeting of the epigenetic and transcriptional machinery), thus, it is likely that a long time would be necessary for a given cell to reach a molecular equilibrium, following continuous overexpression of miR-29a.

Similar to the findings related to miR-29, the association of higher DNMT expression levels with prognostic features of cancer patients is also controversial. For instance, some published works show the association of higher levels of DNMTs with poor prognosis in gastric cancer, AML, and diffuse large B-cell lymphomas,[63–65] whereas in sporadic epithelial ovarian cancer, higher DNMT levels are associated with better OS.[66] Adding complexity, mutations in the DNMT3a are found in a significant fraction of myeloid disorders; nevertheless, a direct link between mutated DNMT3a and downstream epigenetic changes remains to be established.[67,68] In our cohort of T-ALL patients, we did not observe significant differences in clinical/laboratory features or treatment outcome between groups separated based on *DNMT3a*, *DNMT3b*, and *TET1* gene expression levels.

The first reports to describe that altered methylation would play an important role in the physiopathology of T-ALL, with increased methylation of several genes associated with worse prognosis of patients, were published by Roman-Gomez and collaborators.[69–71] Despite suspicions being raised with the retraction of his earlier papers,[69,71] subsequent works corroborated his findings, comprehensively evaluating the impact of methylation status in ALL.[24,72–79]

The complexity associated with epigenetic studies involving miR-29 and its targets is greatly increased by the striking recent findings, describing previously unappreciated roles of DNMT3a and DNMT3b that would also act as 5-hydroxymethylcytosine dehydroxymethylases, as well as 5-methylcytosine demethylases.[80,81]

Another important question relates to the mechanisms leading to the reduced expression levels of miR-29. While this may be explained in AML by the frequently observed deletion of the chromosome 7q32 region, harboring the miR-29a/b1 cluster,[82] or by the commonly observed deficiency of CEBPA (CCAAT/enhancer binding protein alpha), a transactivator of the miR-29a/b1 cluster;[37] in T-ALL, this remains to be explored. Interestingly, one of the mechanisms by which miR-29 family members may become repressed is likely related to the action of the broadly known c-Myc oncogenic transcription factor, as it acts by widely repressing the expression of numerous miRNAs, including miR-29.[83,84] Given that nuclear factor-κB (NF-κB) is constitutively activated in T-ALL cells,[85–87] another mechanism potentially accounting for miR-29 repression in T-ALL may result from the negative regulation exerted by NF-κB on miR-29 transcription,[84] a mechanism that would be probably acting in the downregulation of miR-29, observed in the inflammatory breast cancer subtype.[88] Recently, it was shown that in KIT-driven AML (v-kit Hardy-Zuckerman 4 feline sarcoma viral oncogene homolog, also known as CD117 or Stem Cell Factor Receptor), the KIT mutation drives a MYC-dependent miR-29b repression and increased levels of the miR-29b target Sp1, which forms a complex with NF-κB/HDAC (histone deacetylase), enhancing the expression of SP1 itself and of KIT, further repressing miR-

29b transcription.[89] This intricate network exemplifies the type of signaling that may act in distinct types of cancer, as well as in T-ALL.

Overall, we provide evidence that miR-29a might contribute to the molecular pathophysiology of T-ALL through several newly identified targets, as well as previously identified targets (described in other neoplasias). Moreover, the identification of central components involved in the control of epigenetic dynamics, including *de novo* methylation (such as DNMTs) or active demethylation (such as TET proteins and TDG), adds further complexity to the investigation of miR-29 roles in cancer and leukemia. Finally, we show that miR-29a promotes the demethylation of many genes commonly methylated in T-ALL, indicating that reduced levels of miR-29a may play an important role in the overall methylation status in this hematological malignancy. In light of the recent works showing that *in vivo* delivery of miR-29 mimics may have a potential application in the treatment of AML,[90] further studies are necessary to better understand these complex regulatory circuitries and to eventually translate these findings into potential miR-based therapies.

Acknowledgments

The authors would like to thank Marli H. Tavela, Camila C. B. Menezes, and Augusto Faria for their assistance with laboratory techniques. This work was supported by São Paulo Research Foundation (FAPESP), National Council for Scientific and Technological Development (CNPq), Funding Authority for Studies and Projects (FINEP), Brazil.

Disclosure Statement

The authors have no conflict of interest.

References

1 Bartel DP. MicroRNAs: genomics, biogenesis, mechanism, and function. *Cell* 2004; **116**(2): 281–97.
2 Grimson A, Farh KK, Johnston WK, Garrett-Engele P, Lim LP, Bartel DP. MicroRNA targeting specificity in mammals: determinants beyond seed pairing. *Mol Cell* 2007; **27**(1): 91–105.
3 Guo H, Ingolia NT, Weissman JS, Bartel DP. Mammalian microRNAs predominantly act to decrease target mRNA levels. *Nature* 2010; **466**(7308): 835–40.
4 Shalgi R, Brosh R, Oren M, Pilpel Y, Rotter V. Coupling transcriptional and post-transcriptional miRNA regulation in the control of cell fate. *Aging* 2009; **1**(9): 762–70.
5 Volinia S, Calin GA, Liu CG *et al.* A microRNA expression signature of human solid tumors defines cancer gene targets. *Proc Natl Acad Sci USA* 2006; **103**(7): 2257–61.
6 Garzon R, Heaphy CE, Havelange V *et al.* MicroRNA 29b functions in acute myeloid leukemia. *Blood* 2009; **114**(26): 5331–41.
7 Gebeshuber CA, Zatloukal K, Martinez J. miR-29a suppresses tristetraprolin, which is a regulator of epithelial polarity and metastasis. *EMBO Rep* 2009; **10**(4): 400–5.
8 Pekarsky Y, Croce CM. Is miR-29 an oncogene or tumor suppressor in CLL? *Oncotarget* 2010; **1**(3): 224–7.
9 Lee TY, Ezelle HJ, Venkataraman T, Lapidus RG, Scheibner KA, Hassel BA. Regulation of human RNase-L by the miR-29 family reveals a novel oncogenic role in chronic myelogenous leukemia. *J Interferon Cytokine Res* 2013; **33**(1): 34–42.
10 Calin GA, Liu CG, Sevignani C *et al.* MicroRNA profiling reveals distinct signatures in B cell chronic lymphocytic leukemias. *Proc Natl Acad Sci USA* 2004; **101**(32): 11755–60.
11 Calin GA, Ferracin M, Cimmino A *et al.* A MicroRNA signature associated with prognosis and progression in chronic lymphocytic leukemia. *N Engl J Med* 2005; **353**(17): 1793–801.
12 Zhao JJ, Lin J, Lwin T *et al.* microRNA expression profile and identification of miR-29 as a prognostic marker and pathogenetic factor by targeting CDK6 in mantle cell lymphoma. *Blood* 2010; **115**(13): 2630–9.
13 Zanette DL, Rivadavia F, Molfetta GA *et al.* miRNA expression profiles in chronic lymphocytic and acute lymphocytic leukemia.*Braz J Med Biol Res* 2007; **40**(11): 1435–40.
14 Han YC, Park CY, Bhagat G *et al.* microRNA-29a induces aberrant self-renewal capacity in hematopoietic progenitors, biased myeloid development, and acute myeloid leukemia. *J Exp Med* 2010; **207**(3): 475–89.
15 Picanco-Castro V, Russo-Carbolante E, Reis LC *et al.* Pluripotent reprogramming of fibroblasts by lentiviral mediated insertion of SOX2, C-MYC, and TCL-1A. *Stem Cells Dev* 2011; **20**(1): 169–80.
16 Barrett T, Wilhite SE, Ledoux P *et al.* NCBI GEO: archive for functional genomics data sets–update. *Nucleic Acids Res* 2013; **41**(Database issue): D991–5.
17 Edgar R, Domrachev M, Lash AE. Gene Expression Omnibus: NCBI gene expression and hybridization array data repository. *Nucleic Acids Res* 2002; **30**(1): 207–10.
18 Lewis BP, Burge CB, Bartel DP. Conserved seed pairing, often flanked by adenosines, indicates that thousands of human genes are microRNA targets. *Cell* 2005; **120**(1): 15–20.
19 da Huang W, Sherman BT, Lempicki RA. Systematic and integrative analysis of large gene lists using DAVID bioinformatics resources. *Nat Protoc* 2009; **4**(1): 44–57.
20 da Huang W, Sherman BT, Lempicki RA. Bioinformatics enrichment tools: paths toward the comprehensive functional analysis of large gene lists. *Nucleic Acids Res* 2009; **37**(1): 1–13.
21 Pfaffl MW. A new mathematical model for relative quantification in real-time RT-PCR. *Nucleic Acids Res* 2001; **29**(9): e45.
22 Borgel J, Guibert S, Weber M. Methylated DNA Immunoprecipitation (MeDIP) from Low Amounts of Cells. *Methods Mol Biol* 2012; **925**: 149–58.
23 Weber M, Davies JJ, Wittig D *et al.* Chromosome-wide and promoter-specific analyses identify sites of differential DNA methylation in normal and transformed human cells. *Nat Genet* 2005; **37**(8): 853–62.
24 Kuang SQ, Tong WG, Yang H *et al.* Genome-wide identification of aberrantly methylated promoter associated CpG islands in acute lymphocytic leukemia. *Leukemia* 2008; **22**(8): 1529–38.
25 Dalmazzo LF, Jacomo RH, Marinato AF *et al.* The presence of CD56/CD16 in T-cell acute lymphoblastic leukaemia correlates with the expression of cytotoxic molecules and is associated with worse response to treatment. *Br J Haematol* 2009; **144**(2): 223–9.
26 Garcia-Manero G, Kantarjian HM. The hyper-CVAD regimen in adult acute lymphocytic leukemia. *Hematol Oncol Clin North Am* 2000; **14**(6): 1381–96.
27 Schrappe M, Reiter A, Ludwig WD *et al.* Improved outcome in childhood acute lymphoblastic leukemia despite reduced use of anthracyclines and cranial radiotherapy: results of trial ALL-BFM 90. German-Austrian-Swiss ALL-BFM Study Group. *Blood* 2000; **95**(11): 3310–22.
28 Scrideli CA, Assumpcao JG, Ganazza MA *et al.* A simplified minimal residual disease polymerase chain reaction method at early treatment points can stratify children with acute lymphoblastic leukemia into good and poor outcome groups. *Haematologica* 2009; **94**(6): 781–9.
29 Roehm NW, Rodgers GH, Hatfield SM, Glasebrook AL. An improved colorimetric assay for cell proliferation and viability utilizing the tetrazolium salt XTT. *J Immunol Methods* 1991; **142**(2): 257–65.
30 Svensson SP, Lindgren S, Powell W, Green H. Melanin inhibits cytotoxic effects of doxorubicin and daunorubicin in MOLT 4 cells. *Pigment Cell Res* 2003; **16**(4): 351–4.
31 Villamarin S, Mansilla S, Ferrer-Miralles N, Priebe W, Portugal J. A comparative analysis of the time-dependent antiproliferative effects of daunorubicin and WP631. *Eur J Biochem* 2003; **270**(4): 764–70.
32 Fabbri M, Garzon R, Cimmino A *et al.* MicroRNA-29 family reverts aberrant methylation in lung cancer by targeting DNA methyltransferases 3A and 3B. *Proc Natl Acad Sci USA* 2007; **104**(40): 15805–10.
33 Santanam U, Zanesi N, Efanov A *et al.* Chronic lymphocytic leukemia modeled in mouse by targeted miR-29 expression. *Proc Natl Acad Sci USA* 2010; **107**(27): 12210–15.
34 Mott JL, Kobayashi S, Bronk SF, Gores GJ. mir-29 regulates Mcl-1 protein expression and apoptosis. *Oncogene* 2007; **26**(42): 6133–40.
35 Desjobert C, Renalier MH, Bergalet J *et al.* MiR-29a down-regulation in ALK-positive anaplastic large cell lymphomas contributes to apoptosis blockade through MCL-1 overexpression. *Blood* 2011; **117**(24): 6627–37.
36 Park SY, Lee JH, Ha M, Nam JW, Kim VN. miR-29 miRNAs activate p53 by targeting p85 alpha and CDC42. *Nat Struct Mol Biol* 2009; **16**(1): 23–9.

37 Eyholzer M, Schmid S, Wilkens L, Mueller BU, Pabst T. The tumour-suppressive miR-29a/b1 cluster is regulated by CEBPA and blocked in human AML. *Br J Cancer* 2010; **103**(2): 275–84.
38 Garzon R, Liu S, Fabbri M *et al.* MicroRNA-29b induces global DNA hypomethylation and tumor suppressor gene reexpression in acute myeloid leukemia by targeting directly DNMT3A and 3B and indirectly DNMT1. *Blood* 2009; **113**(25): 6411–18.
39 Yanaihara N, Caplen N, Bowman E *et al.* Unique microRNA molecular profiles in lung cancer diagnosis and prognosis. *Cancer Cell* 2006; **9**(3): 189–98.
40 Nguyen T, Kuo C, Nicholl MB *et al.* Downregulation of microRNA-29c is associated with hypermethylation of tumor-related genes and disease outcome in cutaneous melanoma. *Epigenetics* 2011; **6**(3): 388–94.
41 Bestor TH. The DNA methyltransferases of mammals. *Hum Mol Genet* 2000; **9**(16): 2395–402.
42 Hsieh CL. *In vivo* activity of murine *de novo* methyltransferases, Dnmt3a and Dnmt3b. *Mol Cell Biol* 1999; **19**(12): 8211–18.
43 Okano M, Bell DW, Haber DA, Li E. DNA methyltransferases Dnmt3a and Dnmt3b are essential for *de novo* methylation and mammalian development. *Cell* 1999; **99**(3): 247–57.
44 Bhutani N, Burns DM, Blau HM. DNA demethylation dynamics. *Cell* 2011; **146**(6): 866–72.
45 Garzon R, Volinia S, Liu CG *et al.* MicroRNA signatures associated with cytogenetics and prognosis in acute myeloid leukemia. *Blood* 2008; **111**(6): 3183–9.
46 Zhu C, Wang Y, Kuai W, Sun X, Chen H, Hong Z. Prognostic value of miR-29a expression in pediatric acute myeloid leukemia. *Clin Biochem* 2013; **46**(1–2): 49–53.
47 Griffiths EA, Gore SD. MicroRNA: mIR-ly regulators of DNMT? *Blood* 2009; **113**(25): 6269–70.
48 Wu H, Zhang Y. Mechanisms and functions of Tet protein-mediated 5-methylcytosine oxidation. *Genes Dev* 2011; **25**(23): 2436–52.
49 Lorsbach RB, Moore J, Mathew S, Raimondi SC, Mukatira ST, Downing JR. TET1, a member of a novel protein family, is fused to MLL in acute myeloid leukemia containing the t(10;11)(q22;q23). *Leukemia* 2003; **17**(3): 637–41.
50 Mercher T, Quivoron C, Couronne L, Bastard C, Vainchenker W, Bernard OA. TET2, a tumor suppressor in hematological disorders. *Biochim Biophys Acta* 2012; **1825**(2): 173–7.
51 Moran-Crusio K, Reavie L, Shih A *et al.* Tet2 loss leads to increased hematopoietic stem cell self-renewal and myeloid transformation. *Cancer Cell* 2011; **20**(1): 11–24.
52 Casado FL, Singh KP, Gasiewicz TA. The aryl hydrocarbon receptor: regulation of hematopoiesis and involvement in the progression of blood diseases. *Blood Cells Mol Dis* 2010; **44**(4): 199–206.
53 Mulero-Navarro S, Carvajal-Gonzalez JM, Herranz M *et al.* The dioxin receptor is silenced by promoter hypermethylation in human acute lymphoblastic leukemia through inhibition of Sp1 binding. *Carcinogenesis* 2006; **27**(5): 1099–104.
54 Ge NL, Elferink CJ. A direct interaction between the aryl hydrocarbon receptor and retinoblastoma protein Linking Dioxin Signaling to the Cell Cycle. *J Biol Chem* 1998; **273**(35): 22708–13.
55 Koliopanos A, Kleeff J, Xiao Y *et al.* Increased arylhydrocarbon receptor expression offers a potential therapeutic target for pancreatic cancer. *Oncogene* 2002; **21**(39): 6059–70.
56 Jana NR, Sarkar S, Ishizuka M, Yonemoto J, Tohyama C, Sone H. Cross-talk between 2,3,7,8-tetrachlorodibenzo-p-dioxin and testosterone signal transduction pathways in LNCaP prostate cancer cells. *Biochem Biophys Res Commun* 1999; **256**(3): 462–8.
57 Ito T, Tsukumo S, Suzuki N *et al.* A constitutively active arylhydrocarbon receptor induces growth inhibition of jurkat T cells through changes in the expression of genes related to apoptosis and cell cycle arrest. *J Biol Chem* 2004; **279**(24): 25204–10.
58 Hayashibara T, Yamada Y, Mori N *et al.* Possible involvement of aryl hydrocarbon receptor (AhR) in adult T-cell leukemia (ATL) leukemogenesis: constitutive activation of AhR in ATL. *Biochem Biophys Res Commun* 2003; **300**(1): 128–34.
59 Abdelrahim M, Smith R 3rd, Safe S. Aryl hydrocarbon receptor gene silencing with small inhibitory RNA differentially modulates Ah-responsiveness in MCF-7 and HepG2 cancer cells. *Mol Pharmacol* 2003; **63**(6): 1373–81.
60 Gimenes-Teixeira HL, Lucena-Araujo AR, Dos Santos GA *et al.* Increased expression of miR-221 is associated with shorter overall survival in T-cell acute lymphoid leukemia. *Exp Hematol Oncol* 2013; **2**(1): 10.
61 Yu J, Wang F, Yang GH *et al.* Human microRNA clusters: genomic organization and expression profile in leukemia cell lines. *Biochem Biophys Res Commun* 2006; **349**(1): 59–68.
62 Hu W, Dooley J, Chung SS *et al.* miR-29a maintains mouse hematopoietic stem cell self-renewal by regulating Dnmt3a. *Blood* 2015; **125**(14): 2206–16.
63 Hayette S, Thomas X, Jallades L *et al.* High DNA methyltransferase DNMT3B levels: a poor prognostic marker in acute myeloid leukemia. *PLoS ONE* 2012; **7**(12): e51527.
64 Yang CS, Li Z, Rana TM. microRNAs modulate iPS cell generation. *RNA (New York, NY)* 2011; **17**(8): 1451–60.
65 Amara K, Ziadi S, Hachana M, Soltani N, Korbi S, Trimeche M. DNA methyltransferase DNMT3b protein overexpression as a prognostic factor in patients with diffuse large B-cell lymphomas. *Cancer Sci* 2010; **101**(7): 1722–30.
66 Bai X, Song Z, Fu Y *et al.* Clinicopathological significance and prognostic value of DNA methyltransferase 1, 3a, and 3b expressions in sporadic epithelial ovarian cancer. *PLoS ONE* 2012; **7**(6): e40024.
67 Shah MY, Licht JD. DNMT3A mutations in acute myeloid leukemia. *Nat Genet* 2011; **43**(4): 289–90.
68 Yan XJ, Xu J, Gu ZH *et al.* Exome sequencing identifies somatic mutations of DNA methyltransferase gene DNMT3A in acute monocytic leukemia. *Nat Genet* 2011; **43**(4): 309–15.
69 Roman-Gomez J, Jimenez-Velasco A, Agirre X, Prosper F, Heiniger A, Torres A. Lack of CpG island methylator phenotype defines a clinical subtype of T-cell acute lymphoblastic leukemia associated with good prognosis. *J Clin Oncol* 2005; **23**(28): 7043–9.
70 Roman-Gomez J, Jimenez-Velasco A, Barrios M *et al.* Poor prognosis in acute lymphoblastic leukemia may relate to promoter hypermethylation of cancer-related genes. *Leukemia & Lymphoma* 2007; **48**(7): 1269–82.
71 Roman-Gomez J, Jimenez-Velasco A, Castillejo JA *et al.* Promoter hypermethylation of cancer-related genes: a strong independent prognostic factor in acute lymphoblastic leukemia. *Blood* 2004; **104**(8): 2492–8.
72 Stumpel DJ, Schneider P, van Roon EH *et al.* Specific promoter methylation identifies different subgroups of MLL-rearranged infant acute lymphoblastic leukemia, influences clinical outcome, and provides therapeutic options. *Blood* 2009; **114**(27): 5490–8.
73 Milani L, Lundmark A, Kiialainen A *et al.* DNA methylation for subtype classification and prediction of treatment outcome in patients with childhood acute lymphoblastic leukemia. *Blood* 2010; **115**(6): 1214–25.
74 Davidsson J, Lilljebjorn H, Andersson A *et al.* The DNA methylome of pediatric acute lymphoblastic leukemia. *Hum Mol Genet* 2009; **18**(21): 4054–65.
75 Milani L, Lundmark A, Nordlund J *et al.* Allele-specific gene expression patterns in primary leukemic cells reveal regulation of gene expression by CpG site methylation. *Genome Res* 2009; **19**(1): 1–11.
76 Sato H, Oka T, Shinnou Y *et al.* Multi-step aberrant CpG island hypermethylation is associated with the progression of adult T-cell leukemia/lymphoma. *Am J Pathol* 2010; **176**(1): 402–15.
77 Schafer E, Irizarry R, Negi S *et al.* Promoter hypermethylation in MLL-r infant acute lymphoblastic leukemia: biology and therapeutic targeting. *Blood* 2010; **115**(23): 4798–809.
78 Figueroa ME, Chen SC, Andersson AK *et al.* Integrated genetic and epigenetic analysis of childhood acute lymphoblastic leukemia. *J Clin Investig* 2013; **123**(7): 3099–111.
79 Vilas-Zornoza A, Agirre X, Martin-Palanco V *et al.* Frequent and simultaneous epigenetic inactivation of TP53 pathway genes in acute lymphoblastic leukemia. *PLoS ONE* 2011; **6**(2): e17012.
80 Chen CC, Wang KY, Shen CK. The mammalian *de novo* DNA methyltransferases DNMT3A and DNMT3B are also DNA 5-hydroxymethylcytosine dehydroxymethylases. *J Biol Chem* 2012; **287**(40): 33116–21.
81 Chen CC, Wang KY, Shen CK. DNA 5-methylcytosine demethylation activities of the Mammalian DNA methyltransferases. *J Biol Chem* 2013; **288**(13): 9084–91.
82 Le Beau MM, Espinosa R 3rd, Davis EM, Eisenbart JD, Larson RA, Green ED. Cytogenetic and molecular delineation of a region of chromosome 7 commonly deleted in malignant myeloid diseases. *Blood* 1996; **88**(6): 1930–5.
83 Chang TC, Yu D, Lee YS *et al.* Widespread microRNA repression by Myc contributes to tumorigenesis. *Nat Genet* 2008; **40**(1): 43–50.
84 Mott JL, Kurita S, Cazanave SC, Bronk SF, Werneburg NW, Fernandez-Zapico ME. Transcriptional suppression of mir-29b-1/mir-29a promoter by c-Myc, hedgehog, and NF-kappaB. *J Cell Biochem* 2010; **110**(5): 1155–64.
85 Aifantis I, Vilimas T, Buonamici S. Notches, NFkappaBs and the making of T cell leukemia. *Cell Cycle (Georgetown, Tex)* 2007; **6**(4): 403–6.
86 Mori N, Fujii M, Ikeda S *et al.* Constitutive activation of NF-kappaB in primary adult T-cell leukemia cells. *Blood* 1999; **93**(7): 2360–8.
87 Vilimas T, Mascarenhas J, Palomero T *et al.* Targeting the NF-kappaB signaling pathway in Notch1-induced T-cell leukemia. *Nat Med* 2007; **13**(1): 70–7.
88 Van der Auwera I, Limame R, van Dam P, Vermeulen PB, Dirix LY, Van Laere SJ. Integrated miRNA and mRNA expression profiling of the inflammatory breast cancer subtype. *Br J Cancer* 2010; **103**(4): 532–41.
89 Liu S, Wu LC, Pang J *et al.* Sp1/NFkappaB/HDAC/miR-29b regulatory network in KIT-driven myeloid leukemia. *Cancer Cell* 2010; **17**(4): 333–47.
90 Gong JN, Yu J, Lin HS *et al.* The role, mechanism and potentially therapeutic application of microRNA-29 family in acute myeloid leukemia. *Cell Death Differ* 2014; **21**(1): 100–12.

Supporting Information

Additional supporting information may be found in the online version of this article:

Fig. S1. Evaluation of microRNA-29a (miR-29a) introduction into T-cell acute lymphoblastic leukemia Jurkat cells.

Fig. S2. Effect of microRNA-29a (miR-29a) on transcript levels of selected targets.

Fig. S3. Methylation-specific PCR (MS-PCR) of the *AHR* gene promoter.

Fig. S4. Disease-free survival (A,C,E) and overall survival (B,D,F) in patients with T-cell acute lymphoblastic leukemia.

Table S1. Primer sequences and cycling details for gene expression quantitative PCR.

Table S2. Primer sequences and cycling details for methylated DNA immunoprecipitation (MeDIP) quantitative PCR analysis.

Table S3. MicroRNA-29a (miR-29a) expression in normal and neoplastic cells or tissues.

Table S4. Identified target transcripts and microRNA-29a (miR-29a) binding sites.

Table S5. Identified target transcripts and total number of microRNA-29a (miR-29a) binding sites.

Table S6. Functional analysis of microRNA-29a (miR-29a) targets.

Table S7. Clinical and immunophenotypic features of patients with T-cell acute lymphoblastic leukemia at diagnosis according to expression of DNMT3a, DNMT3b, and TET1.